

## COMMUNICATION

## Radical-Triggered Cross-Linking for Molecular Layer Deposition of SiAlCOH Hybrid Thin Films

Received 00th January 20xx,  
Accepted 00th January 20xx

Kristina Ashurbekova<sup>a</sup>, Karina Ashurbekova<sup>b</sup>, Iva Saric<sup>d</sup>, Evgeny Modin<sup>b</sup>, Mladen Petravić<sup>d</sup>,  
Ilmutdin Abdulagatov<sup>a</sup>, Aziz Abdulagatov<sup>a</sup>, Mato Knez<sup>b,c,d</sup>

DOI: 10.1039/x0xx00000x

**Here, we report on a simultaneous growth and radical-initiated cross-linking of a hybrid thin film in a layer-by-layer manner via molecular layer deposition (MLD). The cross-linked film exhibited a self-limiting MLD growth behavior and improved properties like 12% higher film density and enhanced stability compared to the non-cross-linked film.**

Stable ultrathin organic and hybrid thin films are desirable materials due to their ubiquitous applications. With vapor phase coating processes, the films often grow as arrays of individual molecular chains with limited thermal or mechanical stability. For improving the stability, cross-linking of the chains is the optimal choice.

The outstanding chemical and physical properties of siloxane-based materials, such as high failure to strain, low elastic moduli,<sup>1</sup> or hydrophobicity and chemical inertness<sup>2, 3</sup> have made these materials ubiquitous in science and technology. They found application in microelectronics as dielectric layers,<sup>4, 5</sup> bioinert coatings,<sup>6-8</sup> or thin-film encapsulators.<sup>9</sup> Silicon-based polymers can also be converted into a special class of high-temperature materials known as polymer-derived ceramics (PDCs).<sup>10, 11</sup> Aluminum doped SiOC PDC's, obtained using solution chemistry showed increased creep and corrosion resistance of the final material.<sup>12</sup> For all above-mentioned applications it is beneficial to cross-link the deposited films. The advantages of cross-linking include enhancement of the mechanical strength,<sup>13</sup> thermal stability,<sup>14</sup> and density of the film. Previous studies of siloxane-type films, grown by chemical vapor deposition (CVD), demonstrated the strong dependence of the film stability on the degree of cross-linking.<sup>15</sup> In CVD, the vinyl-functionalized silanes/siloxanes are commonly cross-linked with di-tert-butyl peroxide, cracked into radicals by a hot

filament, as a free-radical-generating initiator.<sup>6</sup> In the case of molecular layer deposition (MLD), cross-linking still remains a challenge. Bent's group demonstrated that a series of multiamines can be used to grow polyurea films by MLD urea-coupling reactions.<sup>16</sup> They showed that the cross-linking indeed improved the film properties. Cross-linking of vinyl groups simultaneous to growing MLD films is a scientific and technical challenge and was not demonstrated so far.

The MLD process is a vapor phase technique developed for organic and hybrid organic-inorganic thin film growth. MLD enables conformal growth of ultrathin and ultrasoother films with molecular level thickness and composition control.<sup>17-20</sup> Siloxane-type films can be grown by MLD. Recently, we have demonstrated the growth of such films following ring-opening polymerization (ROP) reactions of vinyl cyclotrisiloxane (V<sub>3</sub>D<sub>3</sub>) and azasilane.<sup>21</sup> Also, the MLD of a siloxane-alumina hybrid film, using a two-step process including TMA and 2,4,6,8-Tetramethyl-2,4,6,8-tetravinylcyclotetrasiloxane (V<sub>4</sub>D<sub>4</sub>) as precursors, was presented.<sup>22</sup>

In the present work, di-tert-butyl peroxide (TBPO) has been used to perform cross-linking of the V<sub>4</sub>D<sub>4</sub> through their vinyl side chains simultaneously with the growth of the (V<sub>4</sub>D<sub>4</sub>)-TMA alumosiloxane film by MLD.

The proposed schematic of the three-step MLD process is shown in Figure 1. Cross-linking was achieved by introducing a third precursor, TBPO, into the process (Figure 1). The TBPO was dosed after V<sub>4</sub>D<sub>4</sub>, with the pulsing sequence being V<sub>4</sub>D<sub>4</sub>/TBPO/TMA. Reaction (A) represents an anchoring of V<sub>4</sub>D<sub>4</sub> to the aluminum-methylated surface upon ring-opening of V<sub>4</sub>D<sub>4</sub> and binding of the chain to the aluminum through oxygen. In step (B), a thermal decomposition of TBPO occurs,<sup>23</sup> which generates radicals, attacking the vinyl groups on silicon, thereby forming methylene groups and consequently -Si-CHR-CHR-Si-bridges, where R is CH<sub>2</sub>OC(CH<sub>3</sub>)<sub>3</sub> as shown in the inset in Figure 1. The reaction (C) of TMA with the cross-linked V<sub>4</sub>D<sub>4</sub> units occurs in a similar way as in the two-step V<sub>4</sub>D<sub>4</sub>/TMA MLD process.<sup>22</sup> TMA may also attack the C-O-C bonds of the newly formed -CH<sub>2</sub>OC(CH<sub>3</sub>)<sub>3</sub> groups from decomposed TBPO.

<sup>a</sup> Dagestan State University, Makhachkala 36700, Russian Federation.

<sup>b</sup> CIC nanoGUNE, Donostia-San Sebastián E-20018, Spain.

<sup>c</sup> IKERBASQUE, Basque Foundation for Science, Bilbao E-48013, Spain.

<sup>d</sup> University of Rijeka, Department of Physics and Centre for Micro- and Nanosciences and Technologies, 51000 Rijeka, Croatia.

Electronic Supplementary Information (ESI) available: [details of any supplementary information available should be included here]. See DOI: 10.1039/x0xx00000x

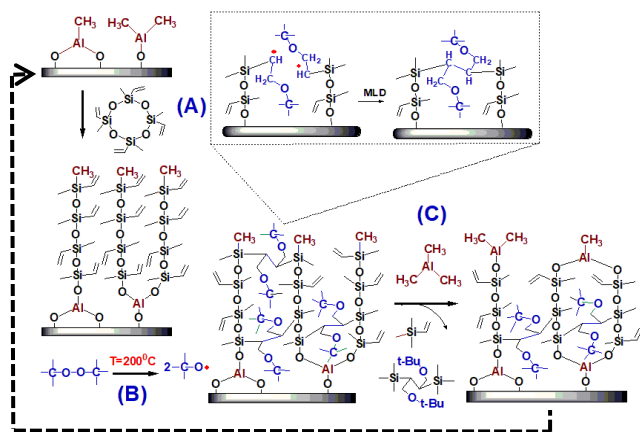


**Figure 1.** Schematic of the alumosiloxane MLD growth from  $V_4D_4$  and TMA, including cross-linking of the chains with di-tert-butyl peroxide (TBPO).

Figure 2 (a) shows the observed QCM mass change vs. time during 20 cycles of  $V_4D_4$ /TBPO/TMA at 200 °C. For the deposition, the 6/22/2/22/2/22 second timing sequence has been used for pulsing and purging of  $V_4D_4$ , TBPO and TMA, respectively. A linear and reproducible mass increase over the MLD cycle numbers was observed. The inset in Figure 2 (a) shows an expanded view of the QCM signal during the three-step MLD process at 200 °C. From the figure, the total mass gain per cycle (MGPC) was 18 ng/cm<sup>2</sup>. The QCM signal shows that each precursor dose results in a mass increase. The  $V_4D_4$ , TBPO and TMA doses lead to a mass gain of 12, 4 and 2 ng/cm<sup>2</sup>, respectively. For QCM studies of the self-limiting surface chemistry of the individual reactions, see Figure 1S in the ESI. Exceeding the dosing times beyond 6, 2 and 2 seconds did not result in a higher mass gain. The mass gain after the TBPO dose is consistent with the proposed reaction mechanism and suggests a radical formation and chain cross-linking. A big spike observed during the TBPO dose is most likely related to a temperature transient<sup>24</sup> and/or TBPO diffusion into the bulk of the MLD film.<sup>25</sup> At 150 °C, we did not observe a mass gain with the TBPO dose, which is likely due to its thermal stability (*viz.* lack of decomposition) at those temperatures (Figure 2S ESI).

Figure 2 (b) shows a comparison of the attenuated total reflectance Fourier transform infrared (ATR-FTIR) spectra of the 400 Å thick film, deposited at 200 °C using a two-step  $V_4D_4$ /TMA MLD, and of the cross-linked 450 Å thick film, deposited at 200 °C using a three-step  $V_4D_4$ /TBPO/TMA MLD process. A background spectrum of pure  $ZrO_2$  nanoparticles was recorded initially and was subtracted from the sample spectra. An intensity decrease of the vinyl signals, such as =CH<sub>2</sub> deformation at 1409 cm<sup>-1</sup>, =CH<sub>2</sub> stretching at 3055 cm<sup>-1</sup>, and =CH stretching at 2930 cm<sup>-1</sup>, can be noticed. The peak at 1460 cm<sup>-1</sup> in the cross-linked film is associated with asymmetric -CH<sub>2</sub> bending from the newly formed methylene groups in the -Si-CHR-CHR-Si- bridges, where R is CH<sub>2</sub>OC(CH<sub>3</sub>)<sub>3</sub>.<sup>26-28</sup> The =CH<sub>2</sub> band at 1409 cm<sup>-1</sup> is still present in the spectrum of the cross-linked film, indicating that not all vinyl groups reacted. Also, this band is attributed to newly generated methylene groups within the film.<sup>6</sup> Another peak at 963 cm<sup>-1</sup> in the cross-linked MLD film is attributed to

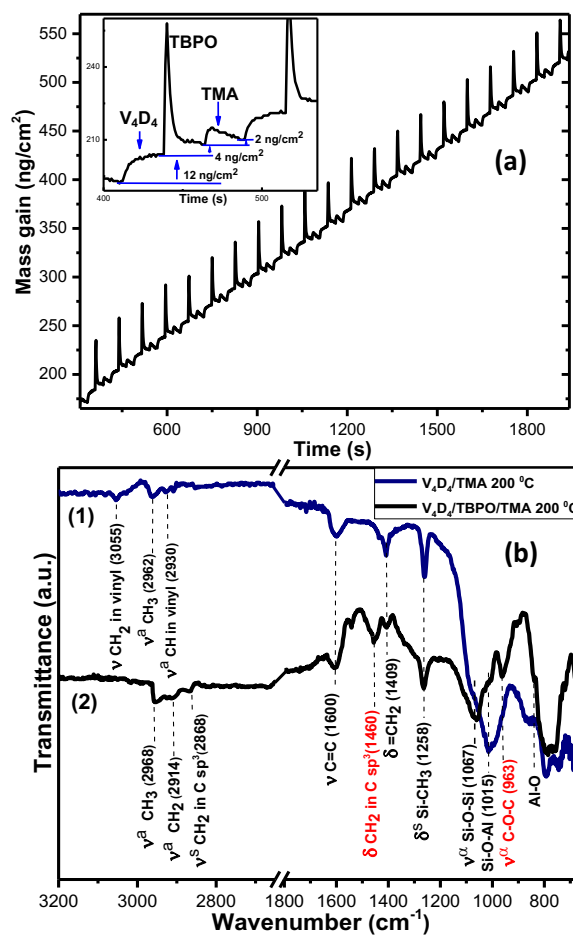


**Figure 2.** (a) QCM mass gain versus time for an MLD process using  $V_4D_4$ , TBPO, and TMA: growth over 20 reaction cycles in a steady-state regime at 200 °C. The inset shows an expanded view of the mass gain during two reaction cycles. (b) ATR-FTIR spectra of (1) 400 Å thick alumosiloxane film, deposited on pressed  $ZrO_2$  particles at 200 °C using a two-step  $V_4D_4$ /TMA MLD; (2) cross-linked 450 Å thick alumosiloxane film, deposited on  $ZrO_2$  particles at 200 °C using a three-step  $V_4D_4$ /TBPO/TMA process.

asymmetric C-O-C stretching vibrations,<sup>29</sup> though the C-O-C stretch typically observed at higher wavenumbers around 1200-1000 cm<sup>-1</sup>. The 1000-1150 cm<sup>-1</sup> region of the spectra (2) is shifted to higher wavenumbers relatively to the spectra (1) on Figure 2. The Si-O-Si peak at 1067 cm<sup>-1</sup>, that appeared on the spectra (1) as a shoulder, appears as a peak on the spectra (2). A small shoulder at 1105 cm<sup>-1</sup> that is seen on the Si-O-Si peak could be the overlapped C-O-C stretch. The appearance of a C-O-C peak is additional evidence of TBPO species incorporation in agreement with the proposed reaction scheme. Other functional groups do not undergo any changes upon the added TBPO step.

A constant growth of 1.8 Å/cycle was obtained for the cross-linked  $V_4D_4$ /TBPO/TMA film deposited on Si(100) at 200 °C. The resulting film density of 2.5 g/cm<sup>3</sup>, as determined from the X-ray reflectivity (XRR) measurements, is 12 % higher than that of the  $V_4D_4$ /TMA film (2.2 g/cm<sup>3</sup>) deposited at the same

temperature, indicating a denser packing of the  $V_4D_4$ /TBPO/TMA film due to the cross-linking. (Figure 3S ESI) A root mean square (RMS) roughness of 5.4 Å was obtained for the 250 Å thick cross-linked aluminosiloxane film. (Figure 3S ESI)

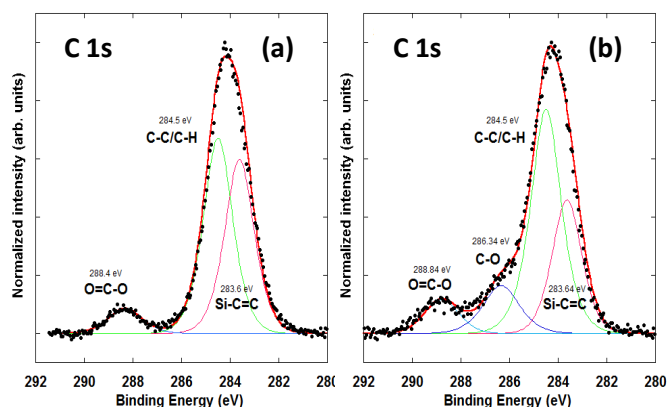


**Figure 3.** XPS spectra around C 1s core-level of (a) a 210 Å thick film deposited at 200 °C using two-step  $V_4D_4$ /TMA process and (b) a cross-linked 240 Å thick film deposited using the three-step  $V_4D_4$ /TBPO/TMA process.

Figure 3 shows a comparison of high-resolution C 1s X-ray photoelectron spectroscopy (XPS) spectra of silicon wafers coated with (a) a 210 Å thick  $V_4D_4$ /TMA film and (b) a cross-linked 240 Å thick  $V_4D_4$ /TBPO/TMA film grown at 200 °C. The spectrum in figure 3 (a) was deconvoluted into three components, assigned to the Si-C=C, C-C/C-H, and O=C-O (surface contamination) bonding arrangement of carbon at BEs of 283.6, 284.5 and 288.8 eV, respectively.<sup>30</sup> A new peak in the spectrum from the cross-linked film in Figure 3 (b) at 286.3 eV is attributed to C-O bonds. This new peak indicates the incorporation of TBPO species into the film and thus cross-linking. The Al 2p and Si 2p spectra of the cross-linked film were identical to those of the  $V_4D_4$ /TMA film.<sup>22</sup>

Finally, transmission electron microscopy (TEM) was used to visualize the conformality of the aluminosiloxane thin film coatings. Figure 4 shows a TEM image of  $ZrO_2$  nanoparticles (NPs) coated with a 55 Å thick cross-linked MLD film, obtained from the three-step  $V_4D_4$ /TBPO/TMA process at 200 °C, using the timing sequence of 6/22/2/22/2/22 to fulfill a self-saturated condition.  $ZrO_2$  NPs were used because of their high surface area and good contrast in TEM. The micrograph in Figure 4 shows conformally coated NPs, confirming a successful MLD process. The growth of 1.75 Å/cycle, as obtained from the TEM image, is in good agreement with the value obtained from XRR, namely 1.8 Å/cycle. The TEM images further confirm the amorphous nature of the deposited film.

The stability of the films was assessed through thermal treatment of the samples and the evaluation of the changes in the film thickness, measured using XRR. Figure 5 shows aluminosiloxane film thickness changes after annealing in air at various temperatures for 1 hour. Annealing of the 150 °C-deposited  $V_4D_4$ /TMA film at 1100 °C resulted in a 47% loss in thickness, while the same thermal treatment of the 200 °C-deposited  $V_4D_4$ /TMA film exhibited a 29% thickness loss. The

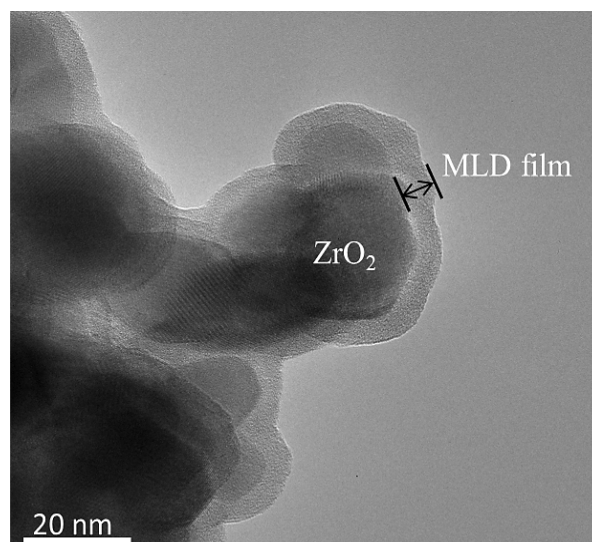


**Figure 4.** TEM image of  $ZrO_2$  NPs coated with 55 Å thick MLD film, deposited using the three-step  $V_4D_4$ /TBPO/TMA process at 200 °C with the timing sequence of 6/22/2/22/2/22.

highest stability was observed from the cross-linked  $V_4D_4$ /TBPO/TMA film, deposited at 200 °C, with only 23% thickness loss after annealing at 1100 °C for 1 hour.

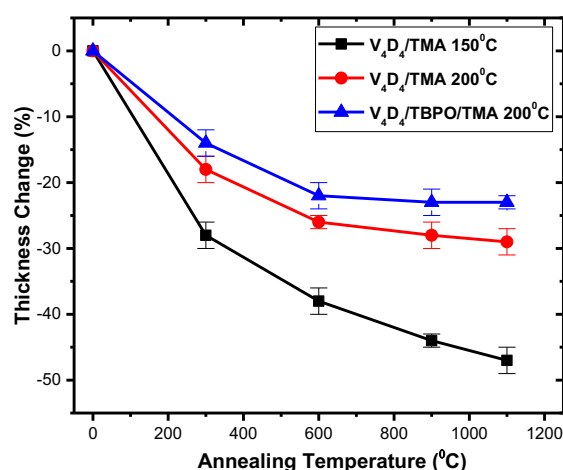


**Figure 5.** Aluminosiloxane film thickness changes after annealing in air at various temperatures for 1 hour. Thickness changes were compared for  $V_4D_4$ /TMA films deposited at 150 °C (black) and 200 °C (red), and cross-linked  $V_4D_4$ /TBPO/TMA deposited at 200 °C (blue).

## Conclusions

In summary, in this study cross-linking of MLD-grown aluminosiloxane films was achieved by introducing a third precursor, di-tert-butyl peroxide (TBPO), into the MLD process at 200 °C processing temperature. A constant growth per cycle and a self-limiting nature of the performed MLD reactions was demonstrated by *in-situ* QCM studies. The presence of characteristic IR peaks of methylene groups in -Si-CHR-CHR-Si-

bridges, where R is CH<sub>2</sub>OC(CH<sub>3</sub>)<sub>3</sub>, as well as an increase in intensity of the C-O component in the XPS C1s spectrum, confirm an effective cross-linking of the vinyl groups by TBPO and the formation of 3D networks in the film. TEM showed a growth of highly conformal films on zirconia nanoparticles. The developed process shows the first MLD-based radical-induced cross-linking approach and is transferrable to other MLD systems that contain chemical groups with unsaturated bonds. The obtained cross-linked MLD film exhibited a thickness loss of 23% after annealing in air at 1100 °C for one hour and 12% higher film density compared to the same film without a cross-linking step. The cross-linking is expected to also enhance the mechanical stability of the deposited films, which is the subject of our ongoing research.

### Author Contributions

The manuscript was written through contributions of all authors. All authors have given approval to the final version of the manuscript.

### Conflicts of interest

There are no conflicts to declare.

### Acknowledgements

M.K. is grateful for funding from the Spanish Ministry of Science and Innovation (MICINN) [Grant Agreement No. PID2019-111065RB-I00], including FEDER funds, and the Maria de Maeztu Units of Excellence Programme [grant number MDM-2016-0618]. Ka.A. acknowledges funding through EU Horizon 2020 research and innovation programme under the Marie Skłodowska-Curie grant agreement No. 765378. I.A. and Kr.A. acknowledge funding through Russian Federation government under the grant number FZNZ-2020-0002. I.S. and M.P. acknowledge support from the University of Rijeka under the project number 18-144.

### References

1. N. Takano, T. Fukuda and K. Ono, *Polymer Journal*, 2001, **33**, 469-474.
2. H. Zhou and S. F. Bent, *The Journal of Physical Chemistry C*, 2013, **117**, 19967-19973.
3. R. G. Closser, D. S. Bergsman and S. F. Bent, *ACS Applied Materials & Interfaces*, 2018, **10**, 24266-24274.
4. H. Moon, H. Seong, W. C. Shin, W.-T. Park, M. Kim, S. Lee, J. H. Bong, Y.-Y. Noh, B. J. Cho, S. Yoo and S. G. Im, *Nature Materials*, 2015, **14**, 628.
5. K. Pak, H. Seong, J. Choi, W. Hwang and S. Im, *Advanced Functional Materials*, 2016, **26**.
6. W. S. O'Shaughnessy, M. Gao and K. K. Gleason, *Langmuir*, 2006, **22**, 7021-7026.
7. W. S. O'Shaughnessy, S. K. Murthy, D. J. Edell and K. K. Gleason, *Biomacromolecules*, 2007, **8**, 2564-2570.
8. A. Achyuta, V. S. Polikov, A. White, H. Pryce Lewis and S. K. Murthy, *Macromolecular bioscience*, 2010, **10**, 872-880.
9. B. Jun Kim, H. Seong, H. Shim, Y. Il Lee and S. Im, *Advanced Engineering Materials*, 2017, **19**.
10. P. Colombo, G. Mera, R. Riedel and G. D. Sorarù, *Journal of the American Ceramic Society*, 2010, **93**, 1805-1837.
11. G. Barroso, Q. Li, R. K. Bordia and G. Motz, *Journal of Materials Chemistry A*, 2019, **7**, 1936-1963.
12. Z. C. Eckel, C. Zhou, J. H. Martin, A. J. Jacobsen, W. B. Carter and T. A. Schaedler, *Science*, 2016, **351**, 58-62.
13. L. Richert, A. J. Engler, D. E. Discher and C. Picart, *Biomacromolecules*, 2004, **5**, 1908-1916.
14. K. Chan and K. K. Gleason, *Langmuir*, 2005, **21**, 8930-8939.
15. D. D. Burkey and K. K. Gleason, *Journal of The Electrochemical Society*, 2004, **151**, F105.
16. H. Zhou, M. F. Toney and S. F. Bent, *Macromolecules*, 2013, **46**, 5638-5643.
17. S. M. George, B. Yoon and A. A. Dameron, *Accounts of Chemical Research*, 2009, **42**, 498-508.
18. K. Ashurbekova, K. Ashurbekova, G. Botta, O. Yurkevich and M. Knez, *Nanotechnology*, 2020, **31**, 342001.
19. G. N. Parsons, S. M. George and M. Knez, *MRS Bulletin*, 2011, **36**, 865-871.
20. X. Meng, *Journal of Materials Chemistry A*, 2017, **5**, 18326-18378.
21. K. Ashurbekova, K. Ashurbekova, I. Saric, E. Modin, M. Petravić, I. Abdulagatov, A. Abdulagatov and M. Knez, *Chemical Communications*, 2020, **56**, 8778-8781.
22. K. Ashurbekova, K. Ashurbekova, I. Saric, M. Gobbi, E. Modin, A. Chuvilin, M. Petravić, I. Abdulagatov and M. Knez, 2020 (Manuscript submitted).
23. Y. Mao and K. K. Gleason, *Langmuir*, 2004, **20**, 2484-2488.
24. M. N. Rocklein and S. M. George, *Analytical Chemistry*, 2003, **75**, 4975-4982.
25. D. Seghete, R. A. Hall, B. Yoon and S. M. George, *Langmuir*, 2010, **26**, 19045-19051.
26. D. Anderson and A. L. Smith, *Wiley-Interscience, New York*, 1974, 247.
27. D. Burkey and K. Gleason, *Journal of Vacuum Science & Technology A - J VAC SCI TECHNOL A*, 2004, **22**, 61-70.
28. S. M. Gates, D. A. Neumayer, M. H. Sherwood, A. Grill, X. Wang and M. Sankarapandian, *Journal of Applied Physics*, 2007, **101**, 094103.
29. D. W. Mayo, F. A. Miller and R. W. Hannah, in *Course Notes on the Interpretation of Infrared and Raman Spectra*, 2003, pp. 73-84.
30. X. Chen, X. Wang and D. Fang, *Fullerenes, Nanotubes and Carbon Nanostructures*, 2020, **28**, 1048-1058.